IEEE Access
Multidisciplinary | Rapid Review | Open Access Journal

Received April 22, 2021, accepted May 4, 2021, date of publication May 6, 2021, date of current version May 17, 2021.

Digital Object Identifier 10.1109/ACCESS.2021.3078115

Optimal Power Flow Solution Using Levy Spiral Flight Equilibrium Optimizer With Incorporating CUPFC

ASHRAF MOSTAFA[1], MOHAMED EBEED[2], SALAH KAMEL[1], AND ABDEL-MOAMEN M. A.[3]

[1]Electrical Engineering Department, Faculty of Engineering, Aswan University, Aswan 81542, Egypt
[2]Electrical Engineering Department, Faculty of Engineering, Sohag University, Sohag 82524, Egypt
[3]Electrical Engineering Department, Faculty of Energy Engineering, Aswan University, Aswan 81528, Egypt

Corresponding authors: Salah Kamel (skamel@aswu.edu.eg) and Abdel-Moamen M. A. (abdelmoamen@energy.aswu.edu.eg)

ABSTRACT Centre Node Unified Power Flow Controller (CUPFC) is a developed member of Flexible Alternating Current Transmission System (FACTS) connected at midpoint of transmission line. It has ability to control the power flow in transmission line (TL) as well as the voltage of the midpoint of TL. Solving the optimal power flow (OPF) problem is crucial task, and it became a difficult problem in case of integration FACTS devices into the system. Therefore, in this paper an efficient optimizer, namely Levy Spiral Flight Equilibrium Optimizer (LSFEO), is proposed for solving the OPF problem and determining the optimal allocation of CUPFC. The proposed algorithm is based on developing the Equilibrium Optimizer (EO) to enhance its searching capabilities. In this technique, two searching strategies are applied to enhance the exploration and exploitation processes of the traditional EO. The first strategy is based on Levy Flight Distribution to enable the optimizer to jump to new search areas for avoiding the stagnation of the traditional EO while the second strategy is based on spiral motion of the particles around the sorted best solution to boost the exploitation. The considered objective functions include fuel cost, fuel cost with valve point effect, emission, voltage deviations and the power losses. The validity and applicability of the proposed algorithm is demonstrated using the IEEE 30-bus system. The simulations verify the superiority of the proposed algorithm over the other reported algorithms. In addition, optimal inclusion of the CUPFC can reduce the cost, VD, losses, and emission considerably.

INDEX TERMS Power system, power flow, optimization, equilibrium optimizer, FACTS, CUPFC.

I. INTRODUCTION

The optimal power flow (OPF) is an important task for the operators and decision makers in electrical power systems. The OPF problem solution means assigning the optimal operating point for reducing the fuel cost, power losses, voltage deviations and emissions as well as enhancing the system stability and loadability. The operating parameters that can accomplish the required objective function are the output powers of the generation units, the voltage of generation systems, the Var output of compensation units and the transformer taps ratio. The OPF problem is a challenge task thus several efforts have been presented for solving this problem. Several traditional methods have been implemented for solving the OPF problem such as linear programming [1], [2], non-linear programming [3], [4], quadratic programming [5], interior point method [6] and Newton-based techniques [7], [8]. The shortages of these methods include suffer from stagnation to local optima for some cases, unstable for solving the nonlinear functions and their unsettled convergence. Therefore, the meta heuristic optimization algorithms have been presented for solving the OPF problem efficiently. Several meta-heuristic algorithms have employed for solving the OPF problem which can be categorized according to their inspiration methods including human based algorithms, physical-based algorithms, and evolutionary based algorithms. Table 1 summarizes these methods for OPF solution.

Equilibrium Optimizer (EO) is new algorithm inspired from control volume mass balance models. EO has

The associate editor coordinating the review of this manuscript and approving it for publication was Tariq Masood.

TABLE 1. Different methods for OPF solution.

Method	Algorithm	Objective function	Ref.
HA	Teaching Learning-Based Optimization	Ploss& Voltage Deviations& Fuel Cost & Stability Index& Piecewise Cost	[9]
	Modified Imperialist Competitive Algorithm	Ploss & Voltage Deviations & Fuel Cost	[10]
	Improved Harmony Search Algorithm	Fuel Cost with Valve Effect	[11]
	Improved Teaching-Learning Based Optimization	Ploss& Voltage Deviations& Fuel Cost & Fuel Cost with VPE& Emission & Piecewise Cost	[12]
	Symbiotic Organisms Search Algorithm	Fuel Cost & Fuel Cost with VPE& Fuel Cost with Prohibited Zones	[13]
EA	Enhanced Self-Adaptive Differential Evolution	Ploss& Fuel Cost & Emission& Stability Index	[14]
	Backtracking search algorithm	Fuel Cost & Fuel Cost with VPE& Fuel Cost with Prohibited Zones	[15]
	Improved Evolutionary Programming	Fuel Cost & Piecewise Cost & Fuel Cost with VPE	[16]
	Evolutionary Programming	Fuel Cost & Piecewise Cost & Fuel Cost with VPE & Voltage Deviations	[17]
	Modified Evolutionary Algorithm-Based Decomposition	Fuel Cost Emission & Stability Index & Voltage Deviations & Ploss	[18]
	Improved Adaptive Differential Evolution	Fuel Cost & Voltage Deviations & Ploss & Emission	[19]
	Genetic Algorithm (GA) Generating Scaling Factor (GSF)	Fuel Cost	[20]
PA	Improved Colliding Bodies Optimization Algorithm	Ploss & Stability Index & Fuel Cost & Fuel Cost with VPE& Emission & Piecewise Cost & Voltage Deviations	[21]
	Opposition Based Gravitational Search Algorithm	Ploss & Fuel Cost & Fuel Cost with VPE& Emission & Stability Index& Piecewise Cost & Voltage Deviations	[22]
	Black-Hole-Based Optimization Approach	Ploss & Voltage Deviations & Fuel Cost & Stability Index	[23]
	Modified Sine-Cosine Algorithm (Msca)	Fuel Cost & Ploss & Voltage Deviations	[24]
	Improved Chaotic Electromagnetic Field Optimization (ICEFO) Algorithm	Fuel Cost & Stability Index & Voltage Deviations	[25]
	Simulated Annealing	Fuel Cost	[26]
SA	Crisscross Search Based Grey Wolf Optimizer	Ploss & Voltage Deviations& Fuel Cost & Fuel Cost with VPE	[27]
	Modified Pigeon-Inspired Optimization Algorithm	Fuel Cost & Fuel Cost with VPE& Ploss & Emission	[28]
	A Joint Self-Adaptive Particle Swarm Optimization (SPSO) And Differential Evolution Algorithms	Fuel Cost & Fuel Cost With VPE& Emission & Piecewise Cost	[25]
	Harris Hawks Optimization	Fuel Cost & Ploss & Emission	[29]
	Developed Grey Wolf Optimizer	Fuel Cost & Fuel Cost with VPE& Emission	[30]
	Modified Grasshopper Optimization	Fuel Cost & Fuel Cost with VPE& Emission & Stability Index& Ploss & Voltage Deviations	[31]
	Improved Moth-Flame Optimization Algorithm	Fuel Cost & Fuel Cost With VPE& Emission & Stability Index& Ploss & Voltage Deviations	[32]
	Improved artificial bee colony optimization algorithm	Fuel Cost & Fuel Cost With VPE& Ploss	[33]

been applied to solve several optimization problems [34]. EO applied for selecting the optimal feature subset for classification problems [35]. EO has been employed for solving the optimal power flow (OPF) problem in hybrid AC/DC power grids [36]. The authors in [37] solved the energy management in a micro-grid under uncertainties of system using the EO. The optimal sizing and sites of renewable distributed generators have been assigned using the EO under uncertainties of several parameters [38].

A. Rabehi *et al.* applied the EO to extract Schottky barrier diodes parameters [39]. In [40], the optimal sizing and sites of biomass distributed generation have been determined using EO.

The unmanned aerial vehicle (UAV) path planning problem has been solve using hybrid EO [41]. The EO has been employed to determine the sizing and placement of the wind turbine-based DG and the Superconducting Magnetic Energy Storage [42].

A CUPFC is an effective controller that is inserted in series at the midpoint of transmission line (TL) to control the voltage magnitude and the power flow through this line [43], [44]. Few publications have been presented to model and assess the effectiveness of this controller where the CUPFC is utilized for improving the power transfer capability of TL [43], [44]. In [45], an efficient transient model of the CUPFC has been introduced to control the power flow in TL. The authors in [46], [47] presented a robust model of the CUPFC into Newton–Raphson power flow method based on power injection model.

In this paper a modified version of EO is proposed for solving the OPF problem and to assign the optimal placement and parameter settings of the CUPFC. The contributions of paper are depicted below.

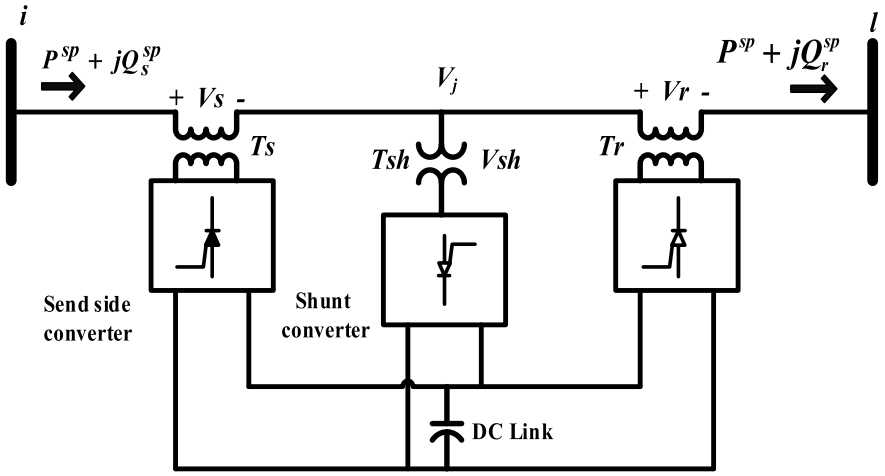

FIGURE 1. Structure of the CUPFC.

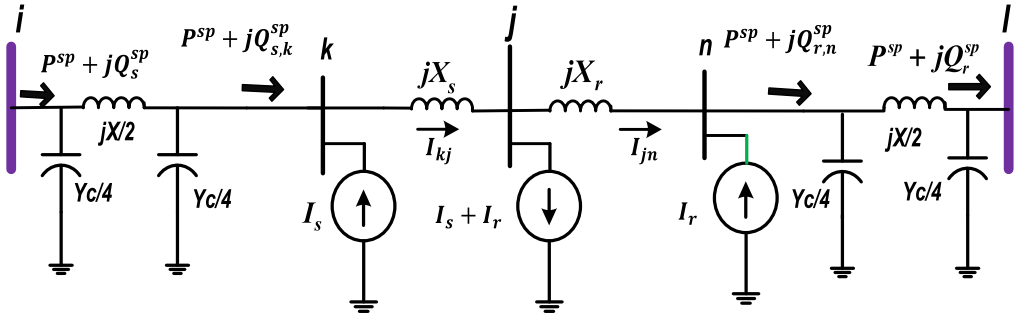

FIGURE 2. Representation of the series converters based on shunt injected current.

- Proposing an enhanced version of Equilibrium Optimizer (EO) namely Levy Spiral Flight Equilibrium Optimizer.
- In the LSFEO, two improvement are used to enhance the performance of the standard EO based on the Levy Flight Distribution and spiral orientation movement of populations.
- Application of the proposed algorithm to solve the OPF problem for different objective functions.
- A simple modeling is used for representing the CUPFC into OPF solution.
- Application of the proposed algorithm to determine the optimal site and size of the CUPFC.
- Assessing the optimal allocation of the CUPFC on power system performance.
- Comparison of the results of LSFEO with standard EO and other optimization algorithms to verify the effectiveness of the proposed algorithm.

The paper is organized as follows: Section 2 presents the modeling and the principal operation of the CUPFC. Section 3 describe the problem formulation. Section explains the EO and LSFEO. Section 4 lists the obtained results and the corresponding discussions of application the LSFEO for OPF solution with CUPFC. The conclusion of this works is depicted in Section 5.

II. MODELING OF CUPFC

A CUPFC is an advanced controller that is incorporated in series at the midpoint of the transmission line. The CUPFC has ability to adjust the active power flow in a TL (P^{sp}), the reactive powers flow at the sending and receiving sides of a TL (Q_s^{sp}, Q_r^{sp}) as well as the midpoint voltage magnitude (V_j). The CUPFC consists of three voltage source converters (VSCs) which connected to the system by three coupling transformers (*Tsh, Tr, Ts*) as shown in Figure 1 [43], [44].

The CUPFC can control the previous parameters by injecting controllable AC voltage to the system. A developed power injection model is used to represent the CUPFC into power flow solution. The power injection model is driven from the voltage source model where the converters of the CUPFC are represented by voltage source (V_s, V_r, V_{sh}) connected in series with their transformer impedances [47]. The series voltage sources are converted to current sources according to (1) and (2) as shown in Figure 2.

$$I_s = \frac{V_s}{jX_s} \tag{1}$$

$$I_r = \frac{V_r}{jX_r} \tag{2}$$

In addition of that the shunt voltage source is presented as generator injects a reactive power only to control the voltage of the midpoint and of that three auxiliary buses are embedded which represents the terminals of the CUPFC.

These currents are calculated as a function of the specified values (P^{sp}, Q_s^{sp}, Q_r^{sp}, V_j) by application the Kirchhoff current law at buses (*j, k, n*) as follows:

KCL at bus k:

$$I_s = I_{kj} - I_{s,k}^{sp} = \frac{V_k - V_j}{jX_s} - \left(\frac{S_{s,k}^{sp}}{V_k}\right)^* \tag{3}$$

where:

$$S_{s,k}^{sp} = P^{sp} + jQ_{s,k}^{sp} \tag{4}$$

$$I_{se1} = -I_{s,k}^{sp} = -\left(\frac{S_{s,k}^{sp}}{V_k}\right)^* \tag{5}$$

$$Q_{s,k}^{sp} = Q_s^{sp} + V_i^2\frac{B}{4} - I_{ik}^2\frac{X}{2} + V_k^2\frac{B}{4} \tag{6}$$

KCL at bus n:

$$I_r = I_{r,n}^{sp} - I_{jn} = \left(\frac{S_{r,n}^{sp}}{V_n}\right)^* - \frac{V_j - V_n}{jX_r} \tag{7}$$

where:

$$I_{se2} = I_{r,n}^{sp} = \left(\frac{S_{r,n}^{sp}}{V_n}\right)^* \tag{8}$$

$$S_{r,n}^{sp} = P^{sp} + jQ_{r,n}^{sp} \tag{9}$$

$$Q_{r,n}^{sp} = Q_r^{sp} - V_l^2\frac{B}{4} + I_{nl}^2\frac{X}{2} - V_n^2\frac{B}{4} \tag{10}$$

The shunt currents are converted to complex loads as follows:

$$S_k = -V_k \times (I_s)^* \tag{11}$$

$$S_n = -V_n \times (I_r)^* \tag{12}$$

$$S_j = V_j \times (I_s + I_r)^* \tag{13}$$

The series-injected voltages can be calculated using (14) and (15) as follows:

$$V_s = -\left(\frac{S_{s,k}^{sp}}{V_k}\right)^* \times jX_s + V_k - V_j \tag{14}$$

$$V_r = \left(\frac{S_{r,n}^{sp}}{V_n}\right)^* \times jX_r - V_j + V_n \tag{15}$$

The injected active powers into the TL from the converters (P_{ex1}, P_{ex2}) can be given using (16) and (17)

$$P_{ex1} = Re\left(V_s\,(I_{se1})^*\right) \tag{16}$$

$$P_{ex2} = Re\left(V_r\,(I_{se2})^*\right) \tag{17}$$

The shunt converter injects apparent power to the system ($P_{sh} + jQ_{sh}$). The main function of P_{sh} is to balance the power through the converters. Thus, P_{sh} is calculated using (18) as follows:

$$P_{sh} = -P_{ex1} - P_{ex2} \tag{18}$$

The injected complex loads at the midpoint node are given as follows:

$$P_j^{load} = P_j - P_{sh} \quad \text{and } Q_j^{load} = Q_j.$$

The injection Q_{sh} by the shunt converter controls the magnitude of the midpoint voltage at the required value. Thus, the midpoint node is represented as a PV bus. The reactive power (Q_{sh}) can be founded using the balanced reactive power at the midpoint as described in (19).

$$\begin{aligned} Q_{sh} = {} & V_j V_k \left(G_{kj}\, sin\, \delta_{kj} - B_{kj}\, cos\, \delta_{ij}\right) \\ & + V_j V_n \left(G_{nj}\, sin\, \delta_{nj} - B_{nj}\, cos\, \delta_{nj}\right) + Q_j^{load} \end{aligned} \tag{19}$$

from Figure 1, the injected V_{sh} and injected I_{sh} are calculated as follows:

$$V_{sh} = V_j + jX_{sh}\left(\frac{P_{sh} + jQ_{sh}}{V_j}\right)^* \tag{20}$$

$$I_{sh} = I_{se1} + I_{se2} \tag{21}$$

From the representation, the proposed model of the CUPFC can be represented by injected complex loads (S_k, S_n, P_j^{load}) and generated reactive power (Q_{sh}) at bus j as depicted in Figure 3.

III. PROBLEM FORMULATION

OPF problem is a convex and nonlinear optimization problem. Generally, the OPF problem can be defined as follows:

$$Minmization\ F(P, H) \tag{22}$$

$$\text{subject to } g_j(P, H) = 0 \quad j = 1, 2, \ldots, m \tag{23}$$

$$h_i(P, H) \le 0 \quad i = 1, 2, \ldots, k \tag{24}$$

where, F represents the objective function, P is a vector represents the control variables, H is a vector of the state variables, g refers to the equality constraints, h refers to the inequality constraints. The P and H vectors are represented as follows:

$$H = \begin{bmatrix} P_{G2} \ldots P_{G,NG}, V_{G1} \ldots V_{G,NG}, Q_{C1} \ldots Q_{C,NC}, \\ T_1 \ldots T_{NT}, P^{sp}, Q_s^{sp}, Q_r^{sp}, V_j \end{bmatrix} \tag{25}$$

$$P = \begin{bmatrix} P_{G1}, V_{L,1} \ldots V_{L,NQ}, Q_{G1} \ldots Q_{G,NG}, \\ S_{TL1} \ldots S_{TL,NTL}, V_s, V_r, V_{sh} \end{bmatrix} \tag{26}$$

where P_G refers to the active power of generator, V_G refers to the voltage magnitude of generator, Q_C refers to the reactive power of capacitors, Q_G refers to the reactive power of generator, V_L refers to load bus voltage, S_{TL} refers to apparent power in TL. NQ, NTL, NG, NC, NT refer to number of the load buses, transmission line, generators, capacitor units and transformers, respectively.

A. OBJECTIVE FUNCTIONS

The considered objective functions in this paper are listed as follows:

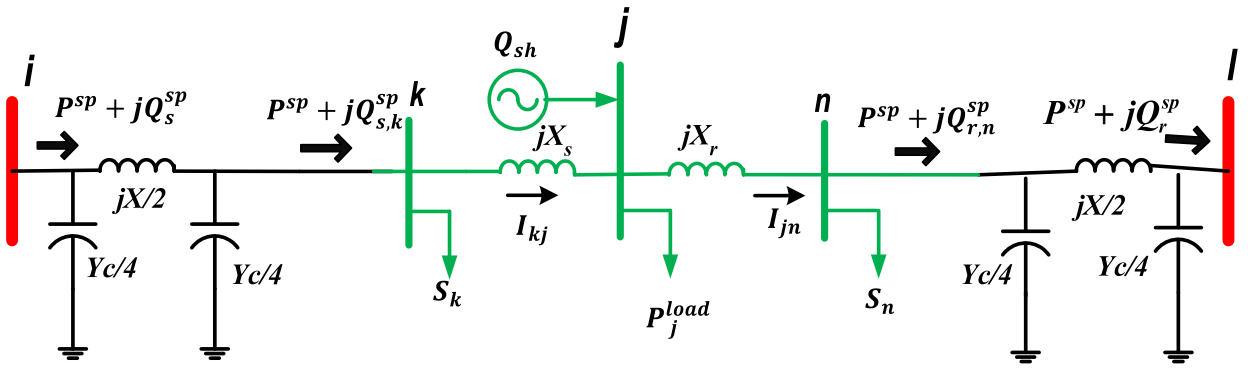

FIGURE 3. The proposed model of the CUPFC.

1) FUEL COST MINIMIZATION

The first considered function is the total production fuel cost, which is described in (27).

$$J_1 = \sum_{i=1}^{NG} \left(a_i + b_i P_{Gi} + c_i P_{Gi}^2\right) \tag{27}$$

where a_i, b_i and c_i denote the cost coefficients.

2) FUEL COST FUNCTION MINIMIZATION WITH VPE

The fuel cost is varied due to change of the steam valves for the steam admission in generators this effect known as the valve point effect (VPE). The VPE are considered in the fuel costs as follows:

$$J_2 = \sum_{i=1}^{NG} \left(a_i + b_i P_{Gi} + c_i P_{Gi}^2\right) + \left|d_i \sin\left(e_i(P_{Gi}^{min} - P_{Gi})\right)\right| \tag{28}$$

where d_i and e_i are the VPE cost coefficients.

3) EMISSION MINIMIZATION

The emission reduction is an important task to diminish the produced of the harmful gases from the generation unit. The emission can be formulated as follows:

$$J_3 = Emission = \sum_{i=1}^{NG} \omega_i P_{Gi}^2 + \sigma_i P_{Gi} + \alpha_i + \zeta_i e^{(\lambda_i P_{Gi})} \tag{29}$$

where ω_i, σ_i, α_i, λ_i and ζ_i denote the emission coefficients.

4) MINIMIZATION FUEL COST, VD AND POWER LOSSES

The fourth objective function is a multi-objective function consists of the fuel cost, the VD and the power losses and it is formulated as follows:

$$J_4 = \left(\sum_{i=1}^{NG} \left(a_i + b_i P_{Gi} + c_i P_{Gi}^2\right)\right) + \omega_1 (VD) + \omega_2 (Ploss) + \omega_3 \left(\sum_{i=1}^{NG} \omega_i P_{Gi}^2 + \sigma_i P_{Gi} + \alpha_i + \zeta_i e^{(\lambda_i P_{Gi})}\right) \tag{30}$$

where,

$$Ploss = \sum_{i=1}^{N_L} G_{ij}(V_i^2 + V_j^2 - 2V_i V_j cos\delta_{ij} \tag{31}$$

$$VD = \sum_{i=1}^{N_Q} |(V_i - 1)| \tag{32}$$

where ω_1, ω_2, and ω_3 denotes to the penalty factors which are selected to be 40,100 and 1000.

B. CONSTRAINTS

1) EQUALITY CONSTRAINTS

$$P_{Gi} - P_{Di} = |V_i| \sum_{j=1}^{NB} |V_j| \left(G_{ij} cos\delta_{ij} + B_{ij} sin\delta_{ij}\right) \tag{33}$$

$$Q_{Gi} - Q_{Di} = |V_i| \sum_{j=1}^{NB} |V_j| \left(G_{ij} cos\delta_{ij} + B_{ij} sin\delta_{ij}\right) \tag{34}$$

where; P_{Di} is the active load, Q_{Di} is the reactive load, G_{ij} is the conductance and B_{ij} are and susceptance of TL, respectively.

2) INEQUALITY CONSTRAINTS

$$\begin{cases} P_{Gn}^{min} \le P_{Gn} \le P_{Gn}^{\max} & n = 1, 2, \ldots, NG \\ V_{Gn}^{min} \le V_{Gn} \le V_{Gn}^{max} & n = 1, 2, \ldots, NG \\ Q_{Gn}^{min} \le Q_{Gn} \le Q_{Gn}^{max} & n = 1, 2, \ldots, NG \\ T_n^{min} \le T_n \le T_n^{max} & n = 1, 2, \ldots, NT \\ Q_{Cn}^{min} \le Q_{Cn} \le Q_{Cn}^{max} & n = 1, 2, \ldots, NC \\ S_{Ln} \le S_{Ln}^{max} & n = 1, 2, \ldots, NTL \\ V_{Ln}^{min} \le V_{Ln} \le V_{Ln}^{max} & n = 1, 2, \ldots, NQ \\ V_S^{min} \le V_s \le V_S^{\max} & \\ V_r^{min} \le V_r \le V_r^{\max} & \\ V_{sh}^{min} \le V_{sh} \le V_{sh}^{\max} & \end{cases} \tag{35}$$

where the min is superscript denotes the minimum boundary of the variable while max is its maximum limit. The objective

function with considering the dependent variable is formulated as follows:

$$\begin{aligned} &J_g(x,u) \\ &= J_i(x,u) + \omega_G\left(P_{G1} - P_{G1}^{lim}\right)^2 + \omega_Q \sum_{n=1}^{NG}\left(Q_{Gn} - Q_{Gn}^{lim}\right)^2 \\ &+ \omega_V \sum_{n=1}^{NQ}\left(V_{Ln} - V_{Ln}^{lim}\right)^2 + \omega_S \sum_{n=1}^{NTL}\left(S_{Ln} - S_{Ln}^{max}\right)^2 \\ &+ \omega_{Vs}\left(V_s - V_s^l im\right)^2 + \omega_{Vr}\left(V_r - V_r^{lim}\right)^2 \\ &+ \omega_{Vsh}\left(V_{sh} - V_{sh}^l im\right)^2 \end{aligned} \tag{36}$$

where ω_G, ω_Q, ω_V, ω_S, ω_{Vs}, ω_{Vr} and ω_{Vsh} are the penalty factors.

$$\begin{cases} If\ P_{G1} > P_{G1}^{max} & then\ P_{G1}^{lim} = P_{G1}^{max} \\ elseIf\ P_{G1} < P_{G1}^{min} & then\ P_{G1}^{lim} = P_{G1}^{min} \end{cases} \tag{37}$$

$$\begin{cases} If\ Q_{Gn} > Q_{Gn}^{max} & then\ Q_{Gn}^{lim} = Q_{Gn}^{max} \\ elseIf\ Q_{Gn} < Q_{Gn}^{min} & then\ Q_{Gn}^{lim} = Q_{Gn}^{min} \end{cases} \tag{38}$$

$$\begin{cases} If\ V_{Ln} > V_{Gn}^{max} & then\ V_{Ln}^{lim} = V_{Gn}^{max} \\ elseIf\ V_{Ln} < V_{Gn}^{min} & then\ V_{Ln}^{lim} = V_{Gn}^{min} \end{cases} \tag{39}$$

$$\begin{cases} If\ V_s > V_S^{\max} & then\ V_s^l im = V_S^{\max} \\ elseIf\ V_s < V_{Gn}^{min} & then\ V_s^{\lim} = V_{Gn}^{min} \end{cases} \tag{40}$$

$$\begin{cases} If\ V_r > V_r^l im & then\ V_r^{lim} = V_r^{\max} \\ elseIf\ V_r < V_r^l im & then\ V_r^{lim} = V_r^{min} \end{cases} \tag{41}$$

$$\begin{cases} If\ V_{sh} > V_{sh}^{\max} & then\ V_{sh}^{lim} = V_{sh}^{\max} \\ elseIf\ V_{sh} < V_{sh}^{min} & then\ V_{sh}^{lim} = V_{sh}^{min} \end{cases} \tag{42}$$

IV. EQUILIBRIUM OPTIMIZER

The equilibrium optimizer (EO) is a new physical based algorithm which is based on the control volume mass balance models to find the equilibrium and dynamic states. In EO, the concentrations represent search agents of the optimization technique. Generally, the volume mass balance model is represented as follows:

$$V\frac{dc}{dt} = QX_{eq} - QX + G \tag{43}$$

where V and X refer to the control volume and the concentration, respectively. While Q is the volumetric flow rate. C represents equilibrium state concentration. By integration of (43), it can be formulated as follows:

$$\begin{aligned} X = X_{eq} + \left(X_0 - X_{eq}\right)\exp\left[-\lambda\left(t - t_0\right)\right] \\ + \frac{G}{\lambda V}\left(1 - \left(\exp\left[-\lambda\left(t - t_0\right)\right]\right)\right) \end{aligned} \tag{44}$$

where, $\lambda = \left(\frac{Q}{V}\right)$. t_0 and C_0 are the initial start time and the initial concentration, respectively. It should be point out here that Eq 44) consists of three parts. The first part denotes to the equilibrium concentration or the equilibrium pool while the second denotes to direct search mechanism which represents the exploration phase of the EO. The third part is related to the generation rate which represents the exploitation phase of this technique. The following steps describe the procedure of the EO:

Step 1: Initialization

In this step a set of concentrations are constructed randomly as follows:

$$X_i^{initial} = X_{min} + rand_i(X_{max} - X_{min}) \quad i = 1, 2, \ldots\ldots n \tag{45}$$

where, C_{max} is maximum limit of the concentration, C_{min} is the minimum limit and $rand_i$ refers to a random value in range [0, 1]. Then, calculate of the objective function of initial concentration.

Step 2: Constructing the equilibrium pool vector

In this step, the concentrations are sorted based on their objective functions. The best four concentration and their average values are selected to be the equilibrium pool vector ($\vec{C}_{eq,pool}$) as follows:

$$X_{eq(avg)} = \frac{X_{eq1} + X_{eq2} + X_{eq3} + X_{eq4}}{4} \tag{46}$$

$$X_{eq,pool} = \left\{X_{eq1}, X_{eq2}, X_{eq3}, X_{eq4}, X_{eq(avg)}\right\} \tag{47}$$

Step 3: Constructing an Exponential Term

In this step an exponential operator (F) is utilized to control the exploration the exploitation abilities of the algorithm. This value will be updated during the iterative process as follows:

$$F = a_1 sign\,(\mathrm{r} - 0.5)\left[e^{-\lambda t} - 1\right] \tag{48}$$

where

$$t = (1 - \frac{T}{T_{Max}})^{(a_2\frac{T}{T_{Max}})} \tag{49}$$

where λ is a random vector within of [0, 1]. a_1 and a_2 denotes to constant factors which are implemented to control the exponential value and they are selected to be 2 and 1, respectively. T_{Max} maximum iteration number while T is the current iterations. It should be highlighted here that a_1 is used to control the exploration phase of the algorithm while a_2 can control the exploitation phase of the EO. sign $(r - 0.5)$ modifies the exploration direction.

Step 4: Application of the generation rate

The generation rate is utilized for updating the concentration and to enhance the exploration phase which is formulated as follows:

$$G = G_0 e^{-k(t-t_0)} \tag{50}$$

where,

$$G_0 = GCP(X_{eq} - \lambda X) \tag{51}$$

$$GCP = \begin{cases} 0.5r_1 & r_2 \geq GP \\ 0 & r_2 < GP \end{cases} \tag{52}$$

where r_1 and r_2 denotes random numbers within range [0, 1]. GCP is a vector formed by the repetition of the same value.

GP refers to the generation probability to control the participation probability of concentration which updated by the generation rate. If $GP = 1$, the generation rate can't participate in the optimization process. If $GP = 0$, the generation rate can participate in the process. GP = 0.5 gives an excellent balancing between exploitation and exploration phases. Referring to the following steps the updated equation of the EO is formulated as follows:

$$X = X_{eq} + \left(X - X_{eq}\right).F + \frac{G}{\lambda V}\left(1 - F\right) \tag{53}$$

Levy Spiral Flight Equilibrium Optimizer: As mentioned before the conventional EO suffer from stagnation for some cases. Thus, a modified version called Levy Spiral Flight Equilibrium Optimizer is proposed for enhancing the searching capability of the conventional EO. The proposed modification is based on two modification Levy flight method and Spiral movement. For enhancing the exploration process of the algorithm, the Levy flight method is implemented to enable the new populations to jump to new areas and to escape from local optima as follows:

$$X_i(k+1) = X_i(k) + \alpha \oplus \text{Lévy}\ (\lambda) \tag{54}$$

where α denotes to the step size, $\oplus$ is the entrywise multiplication. Lévy (λ) is the levy distribution which describe the random walk of the population and it is defined as follows:

$$\text{Lévy}\ (\lambda) \sim u = t^{-\lambda}, \quad (1 < \lambda \leq 3) \tag{55}$$

Lévy (λ) can be specifically calculated using (13) as follows [48]:

$$\text{Lévy}\ (\lambda) \sim \frac{\mu}{|v|^{1/\beta}} \tag{56}$$

where μ and v are random number that can be captured from normal distributions, i.e.,

$$\mu \sim N\left(0, \sigma_\mu^2\right), \quad v \sim N\left(0, \sigma_\mu^2\right) \tag{57}$$

$$\sigma_\mu = \left\{\frac{\Gamma(1+\beta)\sin(\pi\beta/2)}{\Gamma[(1+\beta)/2]\beta 2^{(\beta-1)/2}}\right\}^{1/\beta}, \quad \sigma_v = 1 \tag{58}$$

where Γ denotes the Gamma function while β is a random number in range [0, 2]. In this paper this value is selected to be 1.5 [49]. According to [50], updating concentration based on Lèvy distribution can be expressed as:

$$X_i(k+1) = X_i(k) + \alpha_0 \cdot \frac{\mu}{|v|^{1/\beta}}\left(X_i(k) - X_{eq1}\right) \tag{59}$$

The second improvement that applied to the algorithm is to improve the exploitation of this algorithm at final stage of the iterative process using the spiral movement of the concentration around the best solutions which can be formulated as follows:

$$X_i(k+1) = \left|X_{eq1} - X_i(k)\right| e^{bt} \cos(2\pi t) + XF_i(k) \tag{60}$$

where b is a constant used to control the logarithmic spiral shape. XF_i denotes the sorted concentration at the k-th iteration. To balance between the exploration and the exploitation and adaptive operator is utilized for this action as follows:

$$H(k) = H_{min} + \left(\frac{H_{max} - H_{min}}{T_{Max}}\right) \times k \tag{61}$$

where $\boldsymbol{H_{max}}$ and $\boldsymbol{H_{min}}$ denotes to the minimum and maximum limit of the $\boldsymbol{H}$ operator. $\boldsymbol{T_{Max}}$ denotes the maximum iteration number while $\boldsymbol{k}$ denotes to the current iteration. According to (61) the value of $\boldsymbol{H}$ is changed from its minimum to maximum limit. When the value of $\boldsymbol{H}$ is small, the concentrations will be updated based on levy flight method while when the value of $\boldsymbol{H}$ is closed to its maximum value, the concentrations will be updated using spiral pass movement. The Flow chart of the proposed algorithm for solving the OPF is depicted in Figure 4.

V. SIMULATION RESULTS

In this section, the proposed LSFEO is applied for solving the OPF problem in IEEE 30-bus test system with and without incorporating CUPFC optimally to verify the validity of the proposed algorithm for OPF solution as well as to study the performance of system with optimal inclusion of CUPFC. The single line diagram of this system is shown in Figure 5. In this system number of the generators, lines, transformers, and the VAR compensator units are 6, 41, 4 and 9, respectively. The system load demand is 283.4 MW + j126.2 MVAR and the bus and line data of the system are given in [51]. The voltage limits of generator and load buses are [0.95- 1.1] and [0.95- 1.05], respectively. The shunt VAR compensator rang is [0-5] MVAR and the line limits are founded in [52]. The cost and emission coefficient are depicted in Appendix A. For all studied cases, the empirical parameters of the proposed algorithm are set to be $T_{max} = 100$, Search agents No. = 25, a1 = 2, a2 = 1, GP = 0.5, $H_{max} = 0.9$ and $H_{min} = 0.3$. The studied cases are provided as follows:

A. CASE 1: FUEL COST REDUCTION

In this case the conventional EO and LSFEO are applied to solve the OPF for cost minimization as defined in Eq. (27). The optimal control variables for solving the OPF that obtained by EO and LSFEO are listed in 2nd and 3rd columns, respectively. The value of the fuel costs that obtained by the EO and the LSFEO are 800.2445 \$/h and 799.9519 \$/h, respectively. Thus, the LSFEO is more effective for OPF solution compared with the EO. Table 2 show statistics comparison of the obtained fuel costs by different techniques including SFLA [53], Hybrid SFLA–SA [53], ABC [54], MDE [55], NPSO [56], BSA [15], TS [16], ITS [16], EP [57] and SOS [13]. Judging from Table 2, the minimum fuel cost is obtained by application the proposed algorithm compared with the reported algorithms. Table 3 lists the OPF solution with optimal integration of the CUPFC. In case of incorporating the CUPFC optimally, the fuel cost is reduced to 792.1963\$/h and 791.2974 \$/h by application the EO and the LSFEO, respectively. On other word, the cost is reduced by 8.0482 \$ and 8.6545 \$, respectively. Table 4 lists the locations

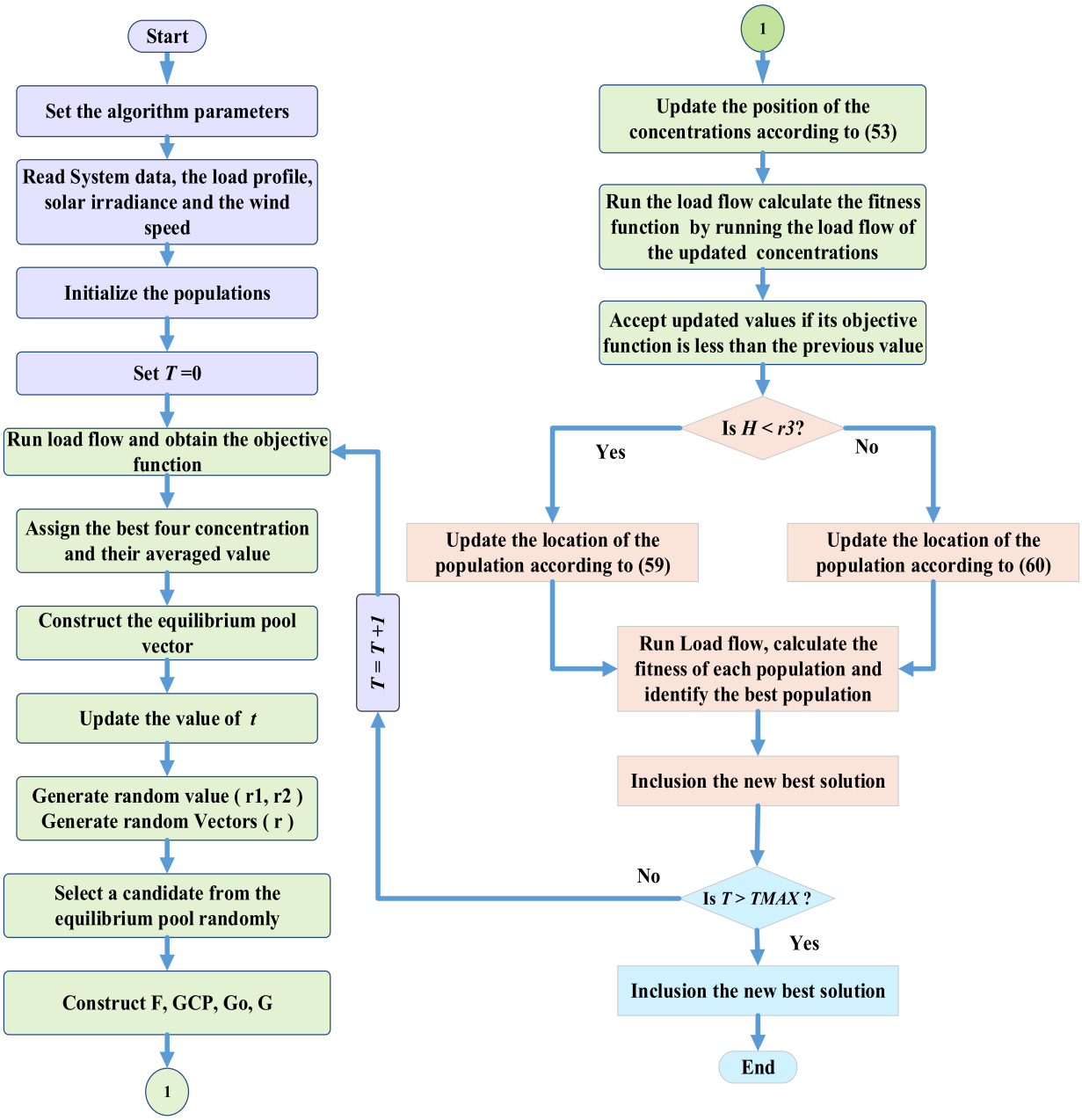

FIGURE 4. Flow chart of the LSFEO for OPF solution.

and the parameter settings of the CUPFC for this case. The optimal location of the CUPFC for this case is at line between buses 1 and 3 while the optimal size and parameter settings are listed in 2nd and 3rd columns of Table 4. The convergence curves of EO and the LSFEO are plotted in Figure 6. It is clear that the LSFEO has stable and smooth convergence nature.

B. CASE 2: FUEL COST REDUCTION WITH VPE

The considered objective function for this case is the cost reduction considering the VPE. The optimal setting of control variables for this case that obtained by EO and LSFEO are listed in 4th and 5th columns of Table1. The minimum fuel costs with application the O and LSFEO are 825.6822 $/h and 824.3207 $/h, respectively. Table 5 shows the statistical comparison of the obtained fuel costs with VPE by different techniques including EO, SFLA [53], Hybrid SFLA–SA [53], ABC [15], BSA [15], PSO [53], SA [53], DE [53], and SOS [13]. Judging from Table 5, the performance of the proposed algorithm is better than the aforementioned algorithms in terms of the best the worst and the average values. In case of incorporating the CUPFC optimally, the fuel cost is reduced to 811.5705 $/h and 810.3275 $/h by application the EO and the LSFEO, respectively. On other word, the cost reduced by 9.2868 $ and 8.9394 $, respectively. The optimal location of

TABLE 2. The optimal results for OPF solution by application EO and LSFEO.

Variables	Case 1 Fuel Cost		Case 2 Fuel Cost with VPE		Case 3 Emission		Case 4 multi objective	
	EO	LSFEO	EO	LSFEO	EO	LSFEO	EO	LSFEO
P1(MW)	177.338	177.418	219.795	219.802	63.887	64.137	83.507	86.254
P2(MW)	48.706	48.314	23.951	28.201	67.894	67.478	63.861	58.960
P5(MW)	21.859	21.275	19.301	15.234	49.998	50.000	41.622	41.867
P8(MW)	21.174	22.566	10.000	10.012	35.000	35.000	35.000	35.000
P11(MW)	11.053	10.570	10.014	10.001	30.000	30.000	29.839	29.994
P13(MW)	12.225	12.123	12.024	12.002	40.000	40.000	33.717	35.445
V1 (p.u.)	1.085	1.078	1.086	1.084	1.053	1.041	1.029	1.036
V2(p.u.)	1.066	1.060	1.060	1.059	1.046	1.034	1.019	1.025
V5(p.u.)	1.028	1.029	1.032	1.025	1.034	1.012	0.993	1.003
V8(p.u.)	1.038	1.034	1.033	1.036	1.028	1.022	0.999	1.008
V11(p.u.)	1.046	1.047	1.054	1.098	1.032	1.020	1.004	0.990
V13 (p.u.)	1.013	1.060	1.034	1.051	1.044	1.076	1.051	1.044
T11	0.961	1.007	0.995	0.975	1.088	0.998	1.058	1.011
T12	1.052	1.001	1.078	1.057	0.992	0.983	0.997	0.995
T15	0.922	0.956	1.014	0.906	1.003	0.911	0.902	0.900
T36	1.013	0.972	0.999	0.977	1.004	0.956	0.949	0.961
QC10(MVAR)	3.383	4.565	0.169	4.352	0.023	4.995	1.631	2.745
QC12(MVAR)	3.066	4.987	1.049	0.486	4.382	1.810	3.256	0.000

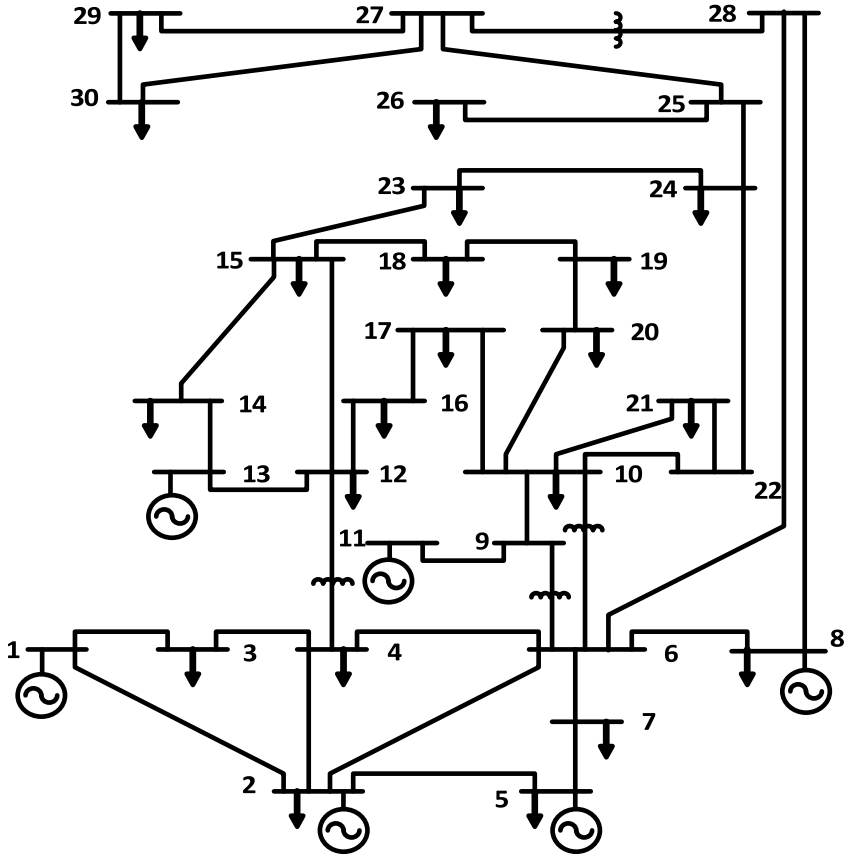

FIGURE 5. Single line diagram of theIEEE-30 bus system.

the CUPFC for this case is at line between buses 1 and 3 while the optimal size and parameter settings are listed in 4th and 5th columns of Table 4. The convergence curves of the EO and the LSFEO are shown in Figure 7. It is clear that the improved LSFEO has stable and smooth convergence nature.

C. CASE 3: EMISSION REDUCTION

The emission reduction is the considered objective function as described in (). The best values for this case that have been obtained by application of the EO and LSFEO are listed in 6th and 7th columns of Table1,

TABLE 3. Statistical results of different algorithms for case 1.

Algorithms	Average	Worst	Best	Time (sec)
LSFEO	**800.4139**	801.7387	**799.9519**	24.22
EO	802.1423	804.2482	800.2445	13.48
Shuffle Frog Leaping Algorithm (SFLA) [53]	NA	NA	801.97	19.22
Shuffle Frog Leaping Algorithm and Simulated Annealing (Hybrid SFLA–SA) [53]	NA	NA	801.79	18.93
Artificial Bee Colony (ABC) [54]	800.8715	801.8674	800.66	NA
Modified Differential Evolution (MDE) [55]	802.382	802.404	802.376	23.25
(NPSO) [56]	800.9024	**801.37**	800.6815	20.45
(BSA) [15]	804	806.37	801.63	NA
Tabu Search (TS) [16]	802.632	802.746	802.502	5173.62
Improved Tabu Search (ITS) [16]	805.812	806.856	804.556	5309.7
Evolutionary Programming (EP) [57]	803.51	805.61	802.62	51.4
Symbiotic Organisms Search Algorithm (SOS) [13]	801.7251	801.8821	801.5733	60.12

TABLE 4. Simulation results with optimal allocation of the CUPFC.

Variables	Case 1: Fuel Cost		Case 2: Fuel Cost with VPE		Case 3: Emission		Case 4: multi objective	
	EO	LSFEO	EO	LSFEO	EO	LSFEO	EO	LSFEO
P1(MW)	178.578	177.839	218.987	219.203	64.048	63.821	92.724	95.164
P2(MW)	48.096	50.509	21.336	22.405	67.676	67.412	56.465	59.974
P5(MW)	21.260	21.566	18.038	17.669	50.000	50.000	44.158	40.173
P8(MW)	17.400	17.255	11.101	10.022	35.000	35.000	35.000	35.000
P11(MW)	12.826	10.741	10.000	10.000	30.000	30.000	30.000	29.949
P13(MW)	12.011	12.025	12.245	12.292	40.000	40.000	28.579	26.801
V1 (p.u.)	1.076	1.065	1.063	1.063	1.003	1.031	1.010	1.003
V2(p.u.)	1.061	1.047	1.044	1.041	0.997	1.025	1.004	1.000
V5(p.u.)	1.023	1.008	1.010	1.009	0.986	0.997	0.989	0.980
V8(p.u.)	1.042	1.026	1.018	1.028	0.999	1.015	1.002	0.993
V11(p.u.)	1.093	1.100	1.030	1.064	0.965	1.100	1.095	0.988
V13 (p.u.)	0.965	1.080	1.083	1.054	1.043	1.100	1.007	1.038
T11	0.924	1.028	1.039	0.978	0.948	1.033	0.917	0.996
T12	1.054	1.025	1.006	1.079	1.021	0.990	0.953	0.978
T15	0.946	0.972	0.912	0.930	0.900	0.940	1.085	0.901
T36	0.994	0.947	0.975	1.012	0.920	0.945	0.935	0.960
QC10(MVAR)	0.973	4.559	0.423	1.551	0.329	4.955	3.146	2.446
QC12(MVAR)	3.382	4.990	4.156	2.792	3.996	0.000	0.000	0.000
QC15(MVAR)	4.965	3.069	2.862	1.674	1.582	4.909	4.568	3.772
QC17(MVAR)	4.592	3.804	0.849	4.164	3.857	2.406	3.277	0.000
QC20(MVAR)	0.781	1.691	3.523	4.721	2.677	0.283	2.145	4.177
QC21(MVAR)	0.689	3.887	2.780	4.508	4.986	3.638	0.811	4.493
QC23(MVAR)	1.684	0.001	4.987	0.201	3.149	0.322	1.478	2.764
QC24(MVAR)	3.108	2.043	4.863	1.793	0.176	0.003	2.840	4.990
QC29(MVAR)	0.657	0.037	3.801	4.991	4.565	4.222	0.373	4.764
Fuel cost($/h)	792.1963	791.2974	815.3611	813.8610	944.7325	943.0823	880.9011	867.7781
Emission(ton/h)	0.3704	0.3693	0.5313	0.5324	0.2049	0.2047	0.2198	0.2232
DDV (p.u.)	0.3590	0.7332	0.5630	0.4371	0.2829	0.6882	0.2106	0.1654
L-max(p.u.)	0.1327	0.1246	0.1241	0.1273	0.1269	0.1258	0.1336	0.1303
Ploss (MW)	6.7707	6.5352	8.3075	8.1913	3.3246	2.8333	3.5256	3.6615

respectively. The minimum emission values that obtained by EO and are 0.2049 ton/h and 0.2048 ton/h, respectively. Table 6 shows the comparison of the obtained the best, the worst and the mean emissions that obtained by different algorithms. According to Table 6 the obtained results by using the LSFEO are better than those obtained by application SKHA [58], KHA [58], ARCBB [59], ABC [60], MTLABO [61] and TLBO [61]. The convergence carves of the EO and LSFEO are shown in Figure 8. It is obvious the proposed algorithm has stable and smooth convergence characteristic.

D. CASE 4: CASE 4: MULTI-OBJECTIVE FUNCTION

In this case is a multi-objective function is considered which includes fuel cost, power loss, voltage deviations and as depicted in (). In case of application the EO, the fuel cost, the VD, the power loss and emissions are 891.4502 $/h, 0.1548 p.u, 4.2121 MW, and 0.2143 ton/h, respectively. With application of the LSFEO, the obtained values of the fuel cost, the VD, the power loss and the emissions are 889.9778 $/h, 0.1645 p.u., 4.1920 MW and 0.2145 ton/h. Therefore, the obtained results by application of the LSFEO are better that those obtained by application the EO in terms

TABLE 5. Optimal setting and sizing of CUPFC for different studied cases (IEEE 30-bus system).

	Case 1		Case 2		Case 3		Case 4	
	EO	LSFEO	EO	LSFEO	EO	LSFEO	EO	LSFEO
Location	(1-3)	(1-3)	(1-3)	(1-3)	(2-6)	(2-6)	(2-5)	(2-5)
$V^{sp}(p.u)$	1.0283	0.9806	1.063	1.006	1.054	0.98	1.0509	0.978
$P^{sp}(MW)$	111.54	106.66	117.29	115.61	54.89	63.23	94.356	92.219
$Q_s^{sp}(MVAR)$	-7.35	-1.72	-23.02	-10.01	28.99	-16.08	35.833	16.317
$Q_r^{sp}(MVAR)$	9.44	-20.18	-5.70	-17.95	32.78	-14.86	54.253	-16.246
$V_s(p.u)$	0.1999 ∠-79.79°	0.2000 ∠-73.0°	0.2000 ∠-80.36°	0.2000 ∠-74.78°	0.0934 ∠-100.41°	0.1332 ∠- 92.21°	0.1731 ∠-90.73°	0.1730 ∠-79.93°
$P_{ex1}(MW)$	2.8000	6.0868	- 0.1505	4.3749	1.9535	-2.3334	0.6327	5.5283
$V_r(p.u)$	0.2000 ∠78.87°	0.1920 ∠89.54°	0.1983 ∠95.92°	0.1915 ∠ 85.21°	0.1301 ∠43.83°	0.1366 ∠ 106.711°	0.1737 ∠87.14°	0.1713 ∠87.72°
$P_{ex2}(MW)$	-2.4528	-4.0348	1.5216	-4.5784	-2.0115	0.1754	-0.2665	-4.7083
$V_{sh}(p.u)$	0.9675 ∠-0.41°	0.9000 ∠-0.50°	1.0656 ∠-0.95°	0.9302 ∠ -1.15°	0.9380 ∠-0.14°	1.0263 ∠0.42°	1.0426 ∠0.25°	0.9000 ∠0.35°
$P_{ex3}(MW)$	- 0.3472	-2.0521	-1.3712	0.2035	0.0581	2.1579	-0.3662	-0.8200

TABLE 6. Statistical results of different algorithms for case 2.

Algorithms	Average	Worst	Best	Time (sec)
LSFEO	825.3482	827.0425	824.3185	21.77
EO	827.9267	836.3878	825.6814	12.26
Shuffle Frog Leaping Algorithm (SFLA) [53]	NA	NA	825.9906126	22.83
Shuffle Frog Leaping Algorithm and Simulated Annealing (Hybrid SFLA–SA) [53]	NA	NA	825.6921669	21.48
(ABC) [15]	NA	NA	825.6	NA
Backtracking Search Algorithm (BSA) [15]	827.69	830.15	825.23	NA
Particle Swarm Optimization (PSO) [53]	NA	NA	826.5897702	24.75
Simulated Annealing (SA) [53]	NA	NA	827.8262923	119.48
Differential Evolution (DE)[53]	NA	NA	826.54	NA
Symbiotic Organisms Search Algorithm (SOS) [13]	825.4039	825.5275	825.2985	120.421

TABLE 7. Statistical results of different algorithms for case 3.

Algorithm	Average	Worst	Best	Time (s)	REF.
Stud Krill Herd Algorithm (SKH)	0.2049	0.2051	0.2048	16.54	[58]
Krill Herd Algorithm	0.2050	0.2054	0.2049	18.02	[58]
Adaptive Real Coded Biogeography-Based Optimization (ARCBBO)	0.2054	0.2064	0.2048	NA	[59]
Artificial Bee Colony (ABC)	NA	NA	0.204826	NA	[60]
Teaching–Learning Based Optimization (TLBO)	NA	NA	0.205	NA	[61]
Modified Teaching–Learning Based Optimization (MTLBO)	NA	NA	0.20493	NA	[61]
Grasshopper Optimizer Algorithm (GOA)	0.20709	0.2128	0.20492	46.17	[62]
Adaptive Grasshopper Optimizer Algorithm (AGOA)	0.204854	0.20487	0.20484	66.51	[62]

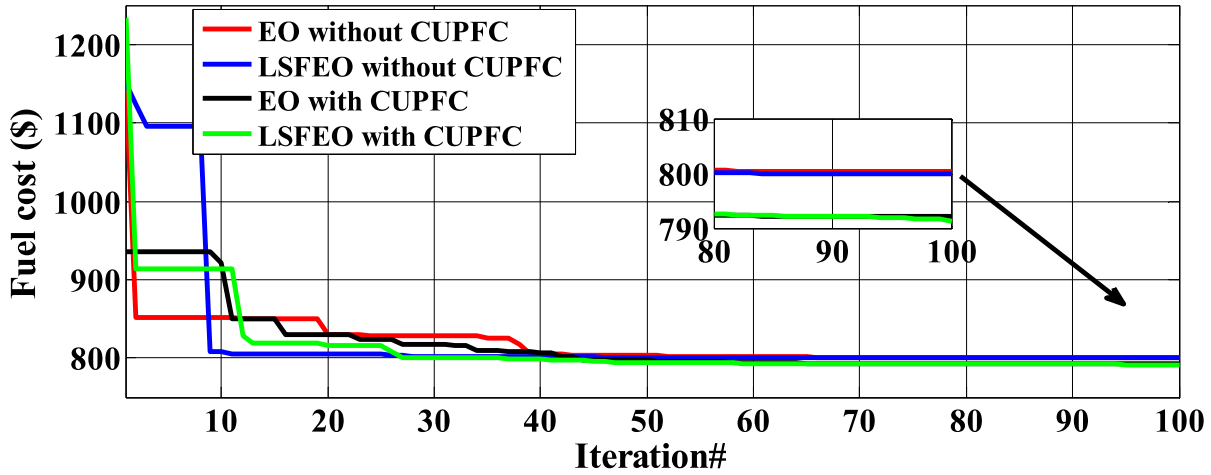

FIGURE 6. The convergence characteristics of EO and LSFEO for case.

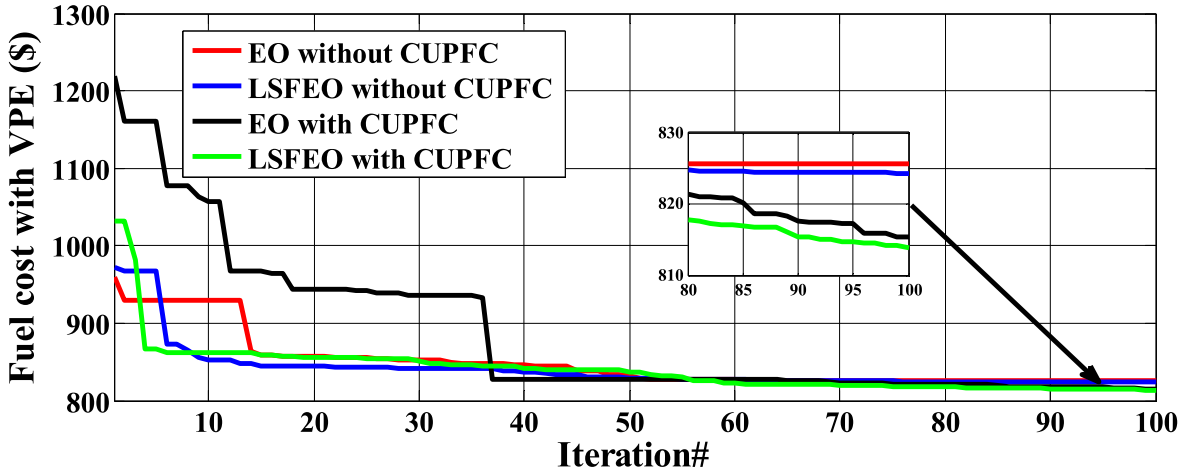

FIGURE 7. The convergence characteristics of EO and LSFEO for case 2.

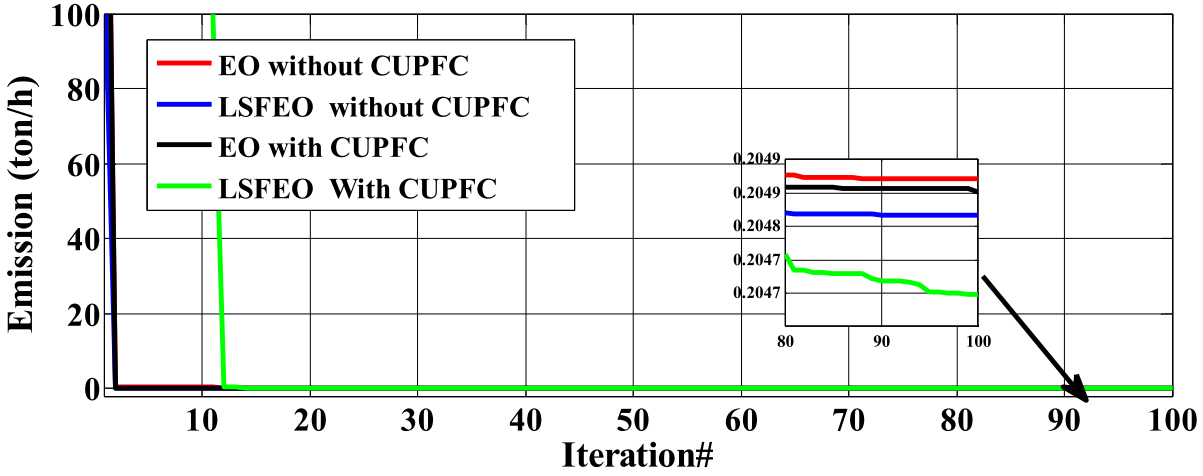

FIGURE 8. The convergence characteristics of EO and LSFEO for case 3.

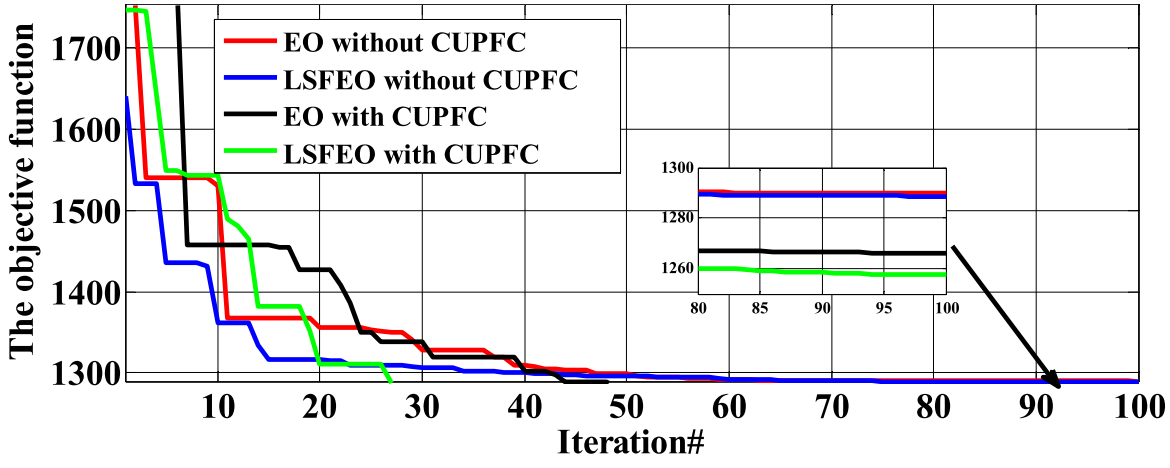

FIGURE 9. The convergence characteristics of EO and LSFEO for case 4.

of the fuel cost, the power loss, and the emissions. In case of optimal inclusion the CUPFC by EO the fuel cost, VD, and power loss are 880.9011 $/h, 0.2106 p.u, 3.5256 MW and 0.2198 MW respectively. while In case of optimal inclusion

the CUPFC by LSFEO the fuel cost, VD, and power loss are 867.7781 $/h, 0.1654 p.u, 3.6615 MW and 0.2232 MW respectively. The convergence curves of EO and the LSFEO for this case are plotted in Figure 9. It is obvious that the LSFEO has stable and smooth convergence nature.

VI. CONCLUSION

This paper has presented an efficient modified version of EO, named Levy Spiral Flight Equilibrium Optimizer for solving the optimal power flow problem and determining the optimal site and size of the CUPFC in the power system. The proposed algorithm is based on two improvements to enhance the searching capabilities of the standard EO. The first suggested improvement is based on the Lèvy motion of the particles to jump to new areas for avoiding the optimizer stagnation and improving the convergence. The second improvement is based on enhancing the exploitation phase of the optimizer by spiral orientation of particles around the best sorted solutions. The proposed algorithm has been implemented on IEEE 30-bus system and the obtained results have been compared with other optimizers. The optimal site and size of the CUPFC have been determined using the LSFEO. The obtained results demonstrated the effectiveness and superiority of the proposed algorithm for OPF problem solution compared with the traditional EO and the state-of-the-art algorithms. In addition, utilizing CUPFC can reduce generation costs, emission, voltage deviations and power losses.

ACKNOWLEDGMENT

The authors gratefully acknowledge the contribution of the NSFC (China)-ASRT (Egypt) Joint Research Fund, Project No. 51861145406 for providing partial research funding to the work reported in this research.

REFERENCES

[1] R. Mota-Palomino and V. H. Quintana, "Sparse reactive power scheduling by a penalty function-linear programming technique," *IEEE Trans. Power Syst.*, vol. PS-1, no. 3, pp. 31–39, Aug. 1986.

[2] T. A. Al-Muhawesh and I. S. Qamber, "The established mega watt linear programming-based optimal power flow model applied to the real power 56-bus system in eastern province of Saudi Arabia," *Energy*, vol. 33, no. 1, pp. 12–21, Jan. 2008.

[3] H. Habibollahzadeh, G.-X. Luo, and A. Semlyen, "Hydrothermal optimal power flow based on a combined linear and nonlinear programming methodology," *IEEE Trans. Power Syst.*, vol. 4, no. 2, pp. 530–537, May 1989.

[4] H. W. Dommel and W. F. Tinney, "Optimal power flow solutions," *IEEE Trans. Power App. Syst.*, vol. PAS-87, no. 10, pp. 1866–1876, Oct. 1968.

[5] R. Burchett, H. Happ, and D. Vierath, "Quadratically convergent optimal power flow," *IEEE Trans. Power App. Syst.*, vol. PAS-103, no. 11, pp. 3267–3275, Nov. 1984.

[6] X. Yan and V. H. Quintana, "Improving an interior-point-based OPF by dynamic adjustments of step sizes and tolerances," *IEEE Trans. Power Syst.*, vol. 14, no. 2, pp. 709–717, May 1999.

[7] D. Sun, B. Ashley, B. Brewer, A. Hughes, and W. Tinney, "Optimal power flow by Newton approach," *IEEE Trans. Power App. Syst.*, vol. PAS-103, no. 10, pp. 2864–2880, Oct. 1984.

[8] A. J. Santos and G. R. M. Da Costa, "Optimal-power-flow solution by Newton's method applied to an augmented Lagrangian function," *IEE Proc.-Gener., Transmiss. Distrib.*, vol. 142, no. 1, pp. 33–36, 1995.

[9] H. R. E. H. Bouchekara, M. A. Abido, and M. Boucherma, "Optimal power flow using teaching-learning-based optimization technique," *Electr. Power Syst. Res.*, vol. 114, pp. 49–59, Sep. 2014.

[10] M. Ghasemi, S. Ghavidel, M. M. Ghanbarian, H. R. Massrur, and M. Gharibzadeh, "Application of imperialist competitive algorithm with its modified techniques for multi-objective optimal power flow problem: A comparative study," *Inf. Sci.*, vol. 281, pp. 225–247, Oct. 2014.

[11] N. Sinsuphan, U. Leeton, and T. Kulworawanichpong, "Optimal power flow solution using improved harmony search method," *Appl. Soft Comput.*, vol. 13, no. 5, pp. 2364–2374, May 2013.

[12] M. Ghasemi, S. Ghavidel, M. Gitizadeh, and E. Akbari, "An improved teaching–learning-based optimization algorithm using Lévy mutation strategy for non-smooth optimal power flow," *Int. J. Electr. Power Energy Syst.*, vol. 65, pp. 375–384, Feb. 2015.

[13] S. Duman, "Symbiotic organisms search algorithm for optimal power flow problem based on valve-point effect and prohibited zones," *Neural Comput. Appl.*, vol. 28, no. 11, pp. 3571–3585, Nov. 2017.

[14] H. Pulluri, R. Naresh, and V. Sharma, "An enhanced self-adaptive differential evolution based solution methodology for multiobjective optimal power flow," *Appl. Soft Comput.*, vol. 54, pp. 229–245, May 2017.

[15] U. Kılıç, "Backtracking search algorithm-based optimal power flow with valve point effect and prohibited zones," *Electr. Eng.*, vol. 97, no. 2, pp. 101–110, Jun. 2015.

[16] W. Ongsakul and T. Tantimaporn, "Optimal power flow by improved evolutionary programming," *Electr. Power Compon. Syst.*, vol. 34, no. 1, pp. 79–95, Jan. 2006.

[17] J. Yuryevich and K. P. Wong, "Evolutionary programming based optimal power flow algorithm," *IEEE Trans. Power Syst.*, vol. 14, no. 4, pp. 1245–1250, Nov. 1999.

[18] J. Zhang, Q. Tang, P. Li, D. Deng, and Y. Chen, "A modified MOEA/D approach to the solution of multi-objective optimal power flow problem," *Appl. Soft Comput.*, vol. 47, pp. 494–514, Oct. 2016.

[19] S. Li, W. Gong, L. Wang, X. Yan, and C. Hu, "Optimal power flow by means of improved adaptive differential evolution," *Energy*, vol. 198, May 2020, Art. no. 117314.

[20] M. Dashtdar, M. Najafi, and M. Esmaeilbeig, "Calculating the locational marginal price and solving optimal power flow problem based on congestion management using GA-GSF algorithm," *Electr. Eng.*, vol. 102, pp. 1–18, Mar. 2020.

[21] H. R. E. H. Bouchekara, A. E. Chaib, M. A. Abido, and R. A. El-Sehiemy, "Optimal power flow using an improved colliding bodies optimization algorithm," *Appl. Soft Comput.*, vol. 42, pp. 119–131, May 2016.

[22] M. H. Sulaiman and Z. Mustaffa, "Solving optimal power flow problem with stochastic wind-solar-small hydro power using barnacles mating optimizer," *Control Eng. Pract.*, vol. 106, Jan. 2021, Art. no. 104672.

[23] S. A. El-Sattar, S. Kamel, M. Ebeed, and F. Jurado, "An improved version of salp swarm algorithm for solving optimal power flow problem," *Soft Comput.*, vol. 25, pp. 1–26, Jan. 2021.

[24] A.-F. Attia, R. A. El Sehiemy, and H. M. Hasanien, "Optimal power flow solution in power systems using a novel sine-cosine algorithm," *Int. J. Electr. Power Energy Syst.*, vol. 99, pp. 331–343, Jul. 2018.

[25] H. Bouchekara, "Solution of the optimal power flow problem considering security constraints using an improved chaotic electromagnetic field optimization algorithm," *Neural Comput. Appl.*, vol. 32, no. 7, pp. 2683–2703, Apr. 2020.

[26] P. J. Vasovala, "Application of ant colony optimization technique in economic load dispatch of IEEE-26 bus system with valve point loading," *Int. J. Res. Appl. Sci. Eng. Technol.*, vol. 9, no. 1, pp. 51–58, Jan. 2021.

[27] A. Meng, C. Zeng, P. Wang, D. Chen, T. Zhou, X. Zheng, and H. Yin, "A high-performance crisscross search based grey wolf optimizer for solving optimal power flow problem," *Energy*, vol. 225, Jun. 2021, Art. no. 120211.

[28] G. Chen, J. Qian, Z. Zhang, and S. Li, "Application of modified pigeon-inspired optimization algorithm and constraint-objective sorting rule on multi-objective optimal power flow problem," *Appl. Soft Comput.*, vol. 92, Jul. 2020, Art. no. 106321.

[29] M. Z. Islam, N. I. A. Wahab, V. Veerasamy, H. Hizam, N. F. Mailah, J. M. Guerrero, and M. N. M. Nasir, "A harris hawks optimization based single- and multi-objective optimal power flow considering environmental emission," *Sustainability*, vol. 12, no. 13, p. 5248, Jun. 2020.

[30] M. Abdo, S. Kamel, M. Ebeed, J. Yu, and F. Jurado, "Solving non-smooth optimal power flow problems using a developed grey wolf optimizer," *Energies*, vol. 11, no. 7, p. 1692, Jun. 2018.

[31] M. A. Taher, S. Kamel, F. Jurado, and M. Ebeed, "Modified grasshopper optimization framework for optimal power flow solution," *Electr. Eng.*, vol. 101, no. 1, pp. 121–148, Apr. 2019.

[32] M. A. Taher, S. Kamel, F. Jurado, and M. Ebeed, "An improved moth-flame optimization algorithm for solving optimal power flow problem," *Int. Trans. Electr. Energy Syst.*, vol. 29, no. 3, p. e2743, Mar. 2019.
[33] W. Bai, I. Eke, and K. Y. Lee, "An improved artificial bee colony optimization algorithm based on orthogonal learning for optimal power flow problem," *Control Eng. Pract.*, vol. 61, pp. 163–172, Apr. 2017.
[34] A. Faramarzi, M. Heidarinejad, B. Stephens, and S. Mirjalili, "Equilibrium optimizer: A novel optimization algorithm," *Knowl.-Based Syst.*, vol. 191, Mar. 2020, Art. no. 105190.
[35] Y. Gao, Y. Zhou, and Q. Luo, "An efficient binary equilibrium optimizer algorithm for feature selection," *IEEE Access*, vol. 8, pp. 140936–140963, 2020.
[36] D. T. Abdul-Hamied, A. M. Shaheen, W. A. Salem, W. I. Gabr, and R. A. El-Sehiemy, "Equilibrium optimizer based multi dimensions operation of hybrid AC/DC grids," *Alexandria Eng. J.*, vol. 59, no. 6, pp. 4787–4803, Dec. 2020.
[37] D. Ahmed, M. Ebeed, A. Ali, A. S. Alghamdi, and S. Kamel, "Multi-objective energy management of a micro-grid considering stochastic nature of load and renewable energy resources," *Electronics*, vol. 10, no. 4, p. 403, Feb. 2021.
[38] A. Ramadan, M. Ebeed, S. Kamel, and L. Nasrat, "Optimal power flow for distribution systems with uncertainty," in *Uncertainties in Modern Power Systems*. Amsterdam, The Netherlands: Elsevier, 2021, pp. 145–162.
[39] A. Rabehi, B. Nail, H. Helal, A. Douara, A. Ziane, M. Amrani, B. Akkal, and Z. Benamara, "Optimal estimation of Schottky diode parameters using a novel optimization algorithm: Equilibrium optimizer," *Superlattices Microstruct.*, vol. 146, Oct. 2020, Art. no. 106665.
[40] A. A. A. El-Ela, S. M. Allam, A. M. Shaheen, and N. A. Nagem, "Optimal allocation of biomass distributed generation in distribution systems using equilibrium algorithm," *Int. Trans. Electr. Energy Syst.*, vol. 31, no. 2, Feb. 2021.
[41] A.-D. Tang, T. Han, H. Zhou, and L. Xie, "An improved equilibrium optimizer with application in unmanned aerial vehicle path planning," *Sensors*, vol. 21, no. 5, p. 1814, Mar. 2021.
[42] M. Hashem, M. Abdel-Salam, M. T. El-Mohandes, M. Nayel, and M. Ebeed, "Optimal placement and sizing of wind turbine generators and superconducting magnetic energy storages in a distribution system," *J. Energy Storage*, vol. 38, Jun. 2021, Art. no. 102497.
[43] B. T. Ooi, M. Kazerani, R. Marceau, Z. Wolanski, F. D. Galiana, D. McGillis, and G. Joos, "Mid-point siting of FACTS devices in transmission lines," *IEEE Trans. Power Del.*, vol. 12, no. 4, pp. 1717–1722, Oct. 1997.
[44] B. Teck Ooi and B. Lu, "C-UPFC: A new FACTS controller with 4 degrees of freedom," in *Proc. IEEE 31st Annu. Power Electron. Spec. Conf.*, vol. 2, Jun. 2000, pp. 961–966.
[45] A. Ajami, S. H. Hosseini, S. Khanmohammadi, and G. B. Gharehpetian, "Modeling and control of C-UPFC for power system transient studies," *Simul. Model. Pract. Theory*, vol. 14, no. 5, pp. 564–576, Jul. 2006.
[46] S. Kamel, F. Jurado, and R. Mihalic, "Advanced modeling of center-node unified power flow controller in NR load flow algorithm," *Electr. Power Syst. Res.*, vol. 121, pp. 176–182, Apr. 2015.
[47] S. Kamel, M. Ebeed, J. Yu, and W. Li, "A comprehensive model of C-UPFC with innovative constraint enforcement techniques in load flow analysis," *Int. J. Electr. Power Energy Syst.*, vol. 101, pp. 289–300, Oct. 2018.
[48] G. Chen, S. Qiu, Z. Zhang, Z. Sun, and H. Liao, "Optimal power flow using gbest-guided cuckoo search algorithm with feedback control strategy and constraint domination rule," *Math. Problems Eng.*, vol. 2017, pp. 1–14, Dec. 2017.
[49] Y. Lin, C. Zhang, and Z. Liang, "Cuckoo search algorithm with hybrid factor using dimensional distance," *Math. Problems Eng.*, vol. 2016, pp. 1–11, Jan. 2016.
[50] X.-S. Yang and S. Deb, "Cuckoo search via Lévy flights," in *Proc. World Congr. Nature Biologically Inspired Comput. (NaBIC)*, 2009, pp. 210–214.
[51] University of Washington. *Power Systems Test Case Archive*. Accessed: Mar. 5, 2021. [Online]. Available: http://www.ee.washington.edu/research/pstca/
[52] S. A. Taher and M. K. Amooshahi, "New approach for optimal UPFC placement using hybrid immune algorithm in electric power systems," *Int. J. Electr. Power Energy Syst.*, vol. 43, no. 1, pp. 899–909, Dec. 2012.
[53] T. Niknam, M. R. Narimani, and R. Azizipanah-Abarghooee, "A new hybrid algorithm for optimal power flow considering prohibited zones and valve point effect," *Energy Convers. Manage.*, vol. 58, pp. 197–206, Jun. 2012.
[54] M. R. Adaryani and A. Karami, "Artificial bee colony algorithm for solving multi-objective optimal power flow problem," *Int. J. Electr. Power Energy Syst.*, vol. 53, pp. 219–230, Dec. 2013.
[55] S. Sayah and K. Zehar, "Modified differential evolution algorithm for optimal power flow with non-smooth cost functions," *Energy Convers. Manage.*, vol. 49, no. 11, pp. 3036–3042, Nov. 2008.
[56] A. I. Selvakumar and K. Thanushkodi, "A new particle swarm optimization solution to nonconvex economic dispatch problems," *IEEE Trans. Power Syst.*, vol. 22, no. 1, pp. 42–51, Feb. 2007.
[57] N. Jayakumar, S. Subramanian, S. Ganesan, and E. B. Elanchezhian, "Grey wolf optimization for combined heat and power dispatch with cogeneration systems," *Int. J. Electr. Power Energy Syst.*, vol. 74, pp. 252–264, Jan. 2016.
[58] H. Pulluri, R. Naresh, and V. Sharma, "A solution network based on stud krill herd algorithm for optimal power flow problems," *Soft Comput.*, vol. 22, no. 1, pp. 159–176, Jan. 2018.
[59] A. R. Kumar and L. Premalatha, "Optimal power flow for a deregulated power system using adaptive real coded biogeography-based optimization," *Int. J. Electr. Power Energy Syst.*, vol. 73, pp. 393–399, Dec. 2015.
[60] M. R. Adaryani and A. Karami, "Artificial bee colony algorithm for solving multi-objective optimal power flow problem," *Int. J. Electr. Power Energy Syst.*, vol. 53, pp. 219–230, Dec. 2013.
[61] A. Shabanpour-Haghighi, A. R. Seifi, and T. Niknam, "A modified teaching–learning based optimization for multi-objective optimal power flow problem," *Energy Convers. Manage.*, vol. 77, pp. 597–607, Jan. 2014.
[62] A. Alhejji, M. E. Hussein, S. Kamel, and S. Alyami, "Optimal power flow solution with an embedded center-node unified power flow controller using an adaptive grasshopper optimization algorithm," *IEEE Access*, vol. 8, pp. 119020–119037, 2020.